Cellular/Molecular

Human $\alpha4\beta2$ Acetylcholine Receptors Formed from Linked Subunits

Yan Zhou, Mark E. Nelson, Alexander Kuryatov, Catherine Choi, John Cooper, and Jon Lindstrom
Department of Neuroscience, University of Pennsylvania Medical School, Philadelphia, Pennsylvania 19104-6074

We prepared concatamers of $\alpha4$ and $\beta2$ subunits for human nicotinic acetylcholine receptors (AChRs), in which the C terminus of $\alpha4$ was linked to the N terminus of $\beta2$, or vice versa, via a tripeptide sequence repeated 6 or 12 times, and expressed them in *Xenopus* oocytes. Linkage did not substantially alter channel amplitude or channel open-duration. Linkage at the C terminus of $\alpha4$ prevented AChR potentiation by 17-β-estradiol by disruption of its binding site. Assembly of AChRs from concatamers was less efficient, but function was much more efficient than that of unlinked subunits. With both linked and free subunits, greater ACh-induced currents per surface AChR were observed with the $(\alpha4)_3(\beta2)_2$ stoichiometry than with the $(\alpha4)_2(\beta2)_3$ stoichiometry. The $(\alpha4)_3(\beta2)_2$ stoichiometry exhibited much lower ACh sensitivity. When concatamers were expressed alone, dipentameric AChRs were formed in which the $(\alpha4)_2(\beta2)_3$ pentamer was linked to the $(\alpha4)_3(\beta2)_2$ pentamer. Dipentamers were selectively expressed on the cell surface, whereas most monopentamers with dangling subunits were retained intracellularly. Coexpression of concatamers with monomeric $\beta2$, $\beta4$, or $\alpha4$ subunits resulted in monopentamers, the stoichiometry of which was determined by the free subunit added. Linkage between the C terminus of $\beta2$ and the N terminus of $\alpha4$ favored formation of ACh-binding sites within the concatamer, whereas linkage between the C terminus of $\alpha4$ and the N terminus of $\beta2$ favored formation of ACh-binding sites between concatamers. These protein-engineering studies provide insight into the structure and function of $\alpha4\beta2$ AChRs, emphasizing the functional differences between $\alpha4\beta2$ AChRs of different stoichiometries.

Key words: **concatamer; nicotinic; receptor; *Xenopus* oocyte; stoichiometry; efficacy**

Introduction

ACh receptors (AChRs) are members of a homologous gene superfamily of ligand-gated ion channels, which includes the $GABA_A$, glycine, and $5\text{-}HT_3$ serotonin receptors (Karlin, 2002). Receptors in the superfamily are formed by five homologous subunits oriented around a central ion channel similar to barrel staves. The predominant AChR subtype in the mammalian brain with high affinity for nicotine is composed of $\alpha4$ and $\beta2$ subunits (Whiting and Lindstrom, 1986, 1987; Zoli et al., 1995). Its stoichiometry has been established as $(\alpha4)_2(\beta2)_3$ when expressed in oocytes using equal amounts of $\alpha4$ and $\beta2$ subunit mRNAs (Anand et al., 1991; Cooper et al., 1991). However, under conditions of limiting $\beta2$ subunits, AChRs with the stoichiometry $(\alpha4)_3(\beta2)_2$ can form (Zwart and Vijverberg, 1998; Nelson et al., 2003). It appears that in the mouse thalamus, there may be a mixture of these two stoichiometries, and an $\alpha4$ A529T polymorphism can alter the ratio of these stoichiometries (Kim et al., 2003). In the $\alpha4$ T529 variant, a greater proportion of the more ACh-sensitive $(\alpha4)_2(\beta2)_3$ stoichiometry was formed. The $\alpha4$ T529 variant is associated with increased sensitivity to nicotine-induced seizures, effects of nicotine on Y-maze activity, respiration rate, and body temperature. The order of subunits around the channel is presumed to be $\alpha4\beta2\alpha4\beta2\beta2$ by homology with the $\alpha1\gamma\alpha1\delta\beta1$ organization of muscle type AChRs (Karlin, 2002). This provides two ACh-binding sites at specific interfaces of $\alpha4$ and $\beta2$ subunits and allows the third $\beta2$, which is not involved in forming an ACh-binding site, to occupy a position equivalent to that of muscle AChR $\beta1$ subunits.

We linked the $\alpha4$ and $\beta2$ subunits via a synthetic oligonucleotide encoding a neutral short peptide to investigate the efficiency of assembly, subunit stoichiometry, and subunit order within an AChR pentamer. Similar approaches have been used to study the $GABA_A$ receptor and potassium channels (Isacoff et al., 1990; Hurst et al., 1992; Liman et al., 1992; Im et al., 1995).

Concatamers were prepared from human $\alpha4$ and $\beta2$ subunits. The C terminus of $\alpha4$ was linked to the N terminus of $\beta2$, or vice versa, via an alanine, glycine, serine (AGS) sequence repeated 6 or 12 times. Dipentameric AChRs were formed from linked subunits. The dipentamers consisted of a pentamer of $(\alpha4)_2(\beta2)_3$ stoichiometry linked to a pentamer of $(\alpha4)_3(\beta2)_2$ stoichiometry. Coexpression with monomeric $\beta2$, $\beta4$, or $\alpha4$ subunits displaced the linked subunits tethering the dipentamers, resulting in monopentamers of one stoichiometry or the other, depending on which native subunit was added in excess. Monopentameric $(\alpha4)_3(\beta2)_2$ AChRs formed by wild-type subunits or a combination of concatamers and free $\alpha4$ subunits produced greater ACh-induced currents per surface AChR than did $(\alpha4)_2(\beta2)_3$ monopentamers formed from wild-type subunits or concatamers in combination with free $\beta2$ subunits. $(\alpha4)_3(\beta2)_2$ AChRs exhibited

Received July 7, 2003; revised Aug. 11, 2003; accepted Aug. 11, 2003.

This work was supported by grants from the National Institutes of Health (NS11323), Smokeless Tobacco Research Council, and Philip Morris External Research Program to J.L. We thank Drs. Gregg B. Wells, Rene Anand, and Volodymyr Gerzanich for valuable comments on this manuscript.

Correspondence should be addressed to Dr. Jon Lindstrom, 217 Stemmler Hall, University of Pennsylvania Medical School, Philadelphia, PA 19104-6074. E-mail: jslkk@mail.med.upenn.edu.

 0270-6474/03/239004-12$15.00/0

Table 1. Linker between the subunits

Name	Concatamer	Sequences of linkers and adjacent subunits showing sites of linker integration (Added amino acids shown in bold)	Linker length (C′ domain + linker + amino acids added in restriction sites = total)
α-12-β	$\alpha4_C$-$(AGS)_{12}$-$_N\beta2$	WLAGMI-**QEGT(AGS)$_{12}$TG**-TEERLV	8 + 36 + 6 = 50
β-6-α	$\beta2_C$-$(AGS)_6$-$_N\alpha4$	SAPSSK-**EG(AGS)$_6$**-RAHAEE	23 + 18 + 2 = 43
α-6-β	$\alpha4_C$-$(AGS)_6$-$_N\beta2$	WLAGMI-**QEGT(AGS)$_6$TG**-TEERLV	8 + 18 + 6 = 32
β-α	$\beta2_C$-$_N\alpha4$	SAPSSK-**EG**-AHAEER	23 + 0 + 2 = 25

much less sensitivity to ACh than did $(\alpha4)_2(\beta2)_3$ AChRs. Variation in $\alpha4\beta2$ AChR subunit stoichiometry is a newly appreciated, biologically important complexity. Linked subunits permit characterization of AChRs of defined subunit stoichiometry and subunit organization.

Materials and Methods

Materials. cDNAs for human α4 (Kuryatov et al., 1997) and β2 (Anand and Lindstrom, 1990) were described previously. Antisera to human α4 were described previously (Kuryatov et al., 2000b), and antisera to β2 were prepared similarly (Kuryatov et al., 2000a). The following subunit-specific monoclonal antibodies (mAbs) were used: mAb 295 to β2 (Whiting and Lindstrom, 1988) and mAb 210 to α1, α3, and α5 (Tzartos et al., 1987; Wang et al., 1996).

Concatamer construction. We prepared tandem constructs of human α4 and β2 AChR subunit cDNAs. The C terminus of α4 was linked to the N terminus of β2, or vice versa, via an AGS sequence repeated 6 or 12 times (encoded by the nucleotide sequence GCT-GGA-AGT). The expression plasmid for the human β2-$(AGS)_6$-α4 concatamer was constructed as follows. First, $(AGS)_6$-α4-**pSP64** was constructed by inserting the $(AGS)_6$ oligo between the signal peptide sequence (MELGGPGA-PRLLPPLLLLLGTGLLRASSHVET) and coding sequence of α4 (starting with RAHAEE) at the *Xma*I and *Apa*I site in α4. Then, a *Stu*I site was introduced into the end of the β2-coding sequence through PCR. Mutated β2-**pSP64** was then digested with both *Sal*I and *Stu*I and then inserted between the *Sal*I and *Sma*I sites in $(AGS)_6$-α4-**pSP64** before an $(AGS)_6$-encoding sequence. The expression plasmid for human β2-α4-**pSP64** was constructed in the same way, except the two subunits were linked directly without any AGS repeat sequences. The signal peptide sequence from β2 was kept in both tandem constructs, whereas the signal peptide sequence of α4 was cleaved during construction.

Expression plasmids for human α4-$(AGS)_6$-β2 and α4-$(AGS)_{12}$-β2 concatamers were constructed as follows. First, β2-**pSP64** was mutated to introduce a *Kpn*I and *Age*I site after the signal peptide sequence (MARRCGPVALLLGFGLLRLCSGVWGTD) and before the coding sequence (starting with TEERLV) of the β2 subunit. Then, $(AGS)_6$-β2-**pSP64** and $(AGS)_{12}$-β2-**pSP64** were constructed by inserting an oligo-encoding $(AGS)_6$ or $(AGS)_{12}$ between the signal peptide sequence and coding sequence of β2 subunit at the *Kpn*I and *Age*I site. A *Kpn*I site was introduced into the end of the α4-coding sequence through PCR. Next, α4-**pSP64** was digested with two sets of enzymes separately. In one case, digestion with both *Sal*I and *Nco*I resulted in a fragment of 1800 bp. Another digestion with both *Nco*I and *Kpn*I resulted in a 218 bp fragment. These two fragments were ligated together into plasmid $(AGS)_6$-β2-**pSP64** or $(AGS)_{12}$-β2-**pSP64** between the *Sal*I and *Kpn*I sites (which is in front of the $(AGS)_6$-encoding sequence). In both cases, the signal peptide sequence from α4 was used.

Oocyte injection. cRNA from linearized cDNA templates for human α4-$(AGS)_6$-β2, α4-$(AGS)_{12}$-β2, β2-$(AGS)_6$-α4, and β2-α4 in the **pSP64** vector were synthesized *in vitro* using SP6 RNA polymerase with mMessage mMachine (Ambion, Austin, TX). *Xenopus* oocytes were injected cytosolically with 10 ng of RNA per oocyte and incubated for 3–5 d in media consisting of 50% L-15 (Invitrogen, San Diego, CA), 10 mM HEPES, pH 7.5, 10 U/ml of penicillin, and 10 μg/ml of streptomycin at 18°C. For all of the experiments in this study, when the wild-type α4β2 or α4β4 AChRs were expressed, 5 ng of α cRNA and 5 ng of β cRNA were injected together in each oocyte. For the expression of all concatamers, if expressed alone, 10 ng of cRNA was injected; if coexpressed with free α or β subunits, 10 ng of concatamer cRNA was used, and 5 ng of α cRNA or β cRNA was injected at the same time.

Surface expression of AChRs formed by concatamers. Surface expression was determined by incubating oocytes in ND-96 solution (96 mM NaCl, 1.8 mM $CaCl_2$, 1 mM $MgCl_2$, 5 mM HEPES, pH 7.5) that contained 10% heat-inactivated normal horse serum and 5 nM β2-specific ^{125}I-mAb 295 (Whiting and Lindstrom, 1988) for 3 hr at room temperature, followed by three wash steps with ice-cold ND-96 solution to remove nonspecifically bound mAbs. Nonspecific binding was determined by incubating noninjected oocytes under similar conditions.

Purification and immunoabsorption of AChRs from oocytes. Oocytes were homogenized by repetitive pipetting in buffer A (50 mM Na_2HPO_4, 50 mM NaCl, 5 mM EDTA, 5 mM EGTA, 5 mM benzamidine, 15 mM iodoacetamide, 2 mM phenylmethylsulfonyl fluoride, 1 μg/ml of pepstatin, pH 7.5) (Gerzanich et al., 1994). The membrane fractions were collected by centrifugation. AChRs were solubilized by incubating membrane fractions of the oocytes in buffer A containing 2% Triton X-100 (buffer C) at 4°C for 1 hr. After removing cellular debris by centrifugation for 20 min at 12,000 × *g*, the cleared extracts were incubated at 4°C for 8–10 hr with 40 μl of mAb 295-coupled Sepharose resin (CH Sepharose 4B resin; Pharmacia, Uppsala, Sweden), which was prepared at 2 mg/ml, according to the instructions of the manufacturer. The resin was collected and then washed three times with buffer A containing 0.5% Triton X-100 (buffer B), washed twice with buffer B that contained 1 M NaCl, and washed twice again with buffer B. The affinity-purified AChR was eluted from the mAb-Sepharose with 3% sodium dodecylsulfate.

Electrophysiology. Three to five days after injection, whole-cell membrane currents were recorded from oocytes injected with various cRNAs using the method described previously (Gerzanich et al., 1995). A two-microelectrode voltage-clamp amplifier (Oocyte Clamp OC-725; Warner Instruments, Hamden, CT) was used to measure currents generated in oocytes in response to the application of agonists. Recordings were analyzed using MacLab software and hardware (ADInstruments,

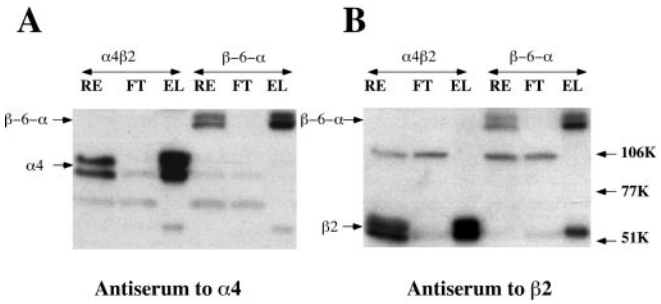

Figure 1. Western blots of wild-type α4 and β2 and the β-6-α construct expressed in oocytes. Proteins from oocytes expressing the wild-type or linked subunits were solubilized in 2% Triton X-100 and then immunopurified on mAb 295-coupled Sepharose CH (Pharmacia) to identify only assembled subunits. The raw extract without purification (RE), the flow through fraction (FT), and the elute (EL) were fractionated by SDS-PAGE and then blotted. Expression of α4, β2, and the concatamer β-6-α were detected by antisera to α4 (*A*) or β2 (*B*) followed by ^{125}I-labeled goat anti-rat IgG (2 nM). After washing, blots were visualized by autoradiography. The α4 blot was autoradiographed for 15 min. The β2 blot was autoradiographed for 60 min. This longer period of exposure resulted in detection of the IgG heavy chain of mAb 295 at 55 kDa in lane EL and a faint unknown band at 106 kDa, which also appears in extracts of uninjected oocytes.

Castle Hill, Australia). To obtain concentration–response relationships, increasing concentrations of ACh were applied to the oocytes at 3 min intervals. The recording chamber was continually perfused with ND-96 with 0.5 μM atropine added to block endogenous muscarinic responses that might remain in oocytes. All recordings were performed at a holding potential of −50 mV. For determination of the relative current amplitudes, 100 μM ACh was applied for 2 sec. The mean current amplitude of at least three oocytes per subunit combination was compared with the mean wild-type α4β2 current amplitude. The same batch of oocytes from each combination was used later to measure the total [^{3}H]epibatidine-binding sites per oocyte. When testing the estrogen effect, 25 μM 17-β-estradiol was made in ND-96 buffer and applied to oocytes for 3 min before exposure to 100 μM ACh. Cytisine efficacy was determined by comparing the maximal response to cytisine for that oocyte to the maximal response measured for ACh. The mean value of the efficacy of at least five oocytes per combination was determined.

Western blots. Triton X-100-solubilized AChRs from oocytes were purified with mAb 295-Sepharose, resolved into subunits by SDS-PAGE, and then transferred to Immun-Blot polyvinylidene difluoride membrane (0.2 μm; Bio-Rad, Hercules, CA). The blots were probed with rat antiserum to α4 (diluted 1:1000) or β2 (diluted 1:500) followed by ^{125}I-labeled goat anti-rat IgG (2 nM). After washing, blots were visualized by autoradiography.

Solid phase RIAs. Immulon 4 (Dynatech, Alexandria, VA) microtiter wells were coated with mAbs as described previously (Anand et al., 1993). Solubilized AChRs from oocytes were prepared as described above and used directly for all assays. mAb-coated microtiter wells were incubated with Triton X-100-solubilized AChRs in the presence of 2 nM [^{3}H]epibatidine (specific activity, 1800 GBq/mmol; PerkinElmer Life Sciences, Emeryville, CA) at 4°C overnight. The wells were then washed three times with ice-cold PBS and 0.05% Tween 20 buffer, and the amount of radioactivity bound was determined by liquid scintillation counting. The nonspecific binding of [^{3}H]epibatidine was determined by processing the RIAs with lysates of noninjected oocytes.

Sucrose gradient sedimentation. Triton-solubilized AChRs from oocytes were prepared as described above. Aliquots (200 μl) of the lysates, mixed with 1 μl of 1 mg/ml of pure extract of *Torpedo californica* electric organ, were loaded onto 5 ml of sucrose gradients [linear 5–20% sucrose (w/w) in 10 mM sodium phosphate buffer, pH 7.5, which contained 100 mM NaCl, 1 mM NaN_3, and 0.5% Triton X-100]. The gradients were centrifuged for 1 hr at 70,000 rpm in a Beckman NVT-90 rotor (Beckman Instruments, Fullerton, CA) at 4°C. The fractions were collected at 11 drops per well from the bottom of the tubes and used for additional analysis. If the fractions were to be analyzed by RIAs, they were collected directly in mAb 295-coated wells first and then 5 μl of each fraction was transferred to mAb 210-coated wells to measure the *Torpedo* AChR standard profile. Fractions in mAb 295-coated wells were incubated with 5 nM [^{3}H]epibatidine at 4°C overnight, whereas fractions in mAb 210-coated wells were incubated with 2 nM ^{125}I-α-bungarotoxin at 4°C overnight. Afterward, the wells were washed three times with PBS and 0.05% Tween 20, and the bound [^{3}H]epibatidine was determined by liquid scintillation counting, whereas the bound ^{125}I-α-bungarotoxin was determined by γ-counting.

Sucrose gradient sedimentation of surface AChRs. Oocytes were first washed three times with PBS (100 mM NaCl, 10 mM sodium phosphate buffer, pH 7.0) buffer and then incubated in PBS buffer that contained 0.5 mg/ml of EZ-link sulfo-NHS-SS-Biotin (Pierce, Rockford, IL) at room temperature for 30 min to label the surface proteins. After incubation, oocytes were gently washed three times in PBS buffer. Triton-solubilized AChRs from oocytes were prepared as described previously. A sucrose gradient was run following the protocol described above. Immulon 4 (Dynatech) microtiter wells were coated with streptavidin (Sigma, St. Louis, MO) at a final concentration of 10 μg/ml as described previously (Anand et al., 1993). After centrifugation, fractions were collected in mAb 295-coated wells first, and then 5 μl of each fraction was transferred to mAb 210-coated wells to determine the *Torpedo* AChR profile, and 60 μl of each fraction was transferred to streptavidin-coated wells. Fractions in mAb 295-coated wells and streptavidin-coated wells were both incubated with 5 nM [^{3}H]epibatidine at 4°C overnight to measure the amount of epibatidine-binding sites for total and surface AChRs.

Single-channel analyses. Single-channel data were acquired and analyzed as described in detail by Nelson and Lindstrom (1999). In brief, oocytes were prepared as described above and monitored for expression by application of a saturating concentration of ACh while under voltage clamp. Eggs with adequate expression were prepared for patch-clamp recording by manual removal of the vitelline membrane after osmotic shrinkage (Methfessel et al., 1986). Outside-out patches were formed

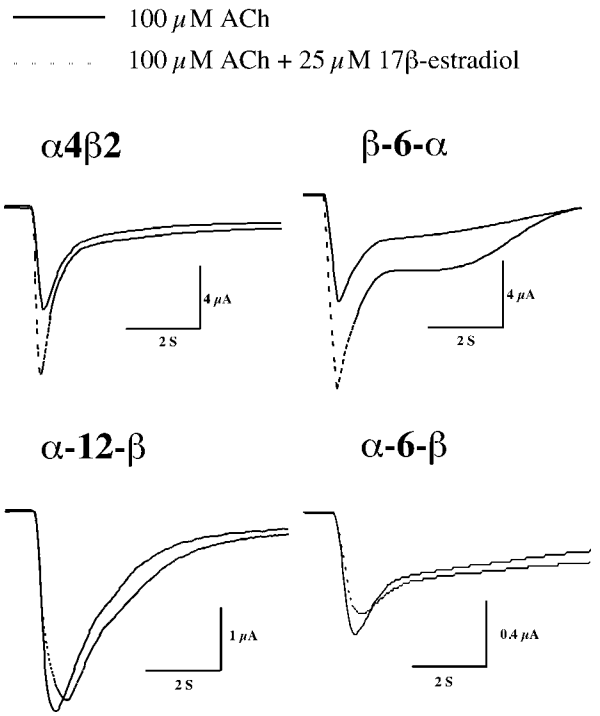

Figure 2. Concatamer β-6-α could be potentiated by estrogenic steroid, whereas concatamer α-6-β and α-12-β were not. 17-β-estradiol (25 μM) was made in ND-96 buffer and used to wash oocytes for 3 min before applying ACh (100 μM). Concatamer β-6-α, with an unaltered C terminus, was potentiated by 17-β-estradiol, just as the wild-type α4β2 AChRs.

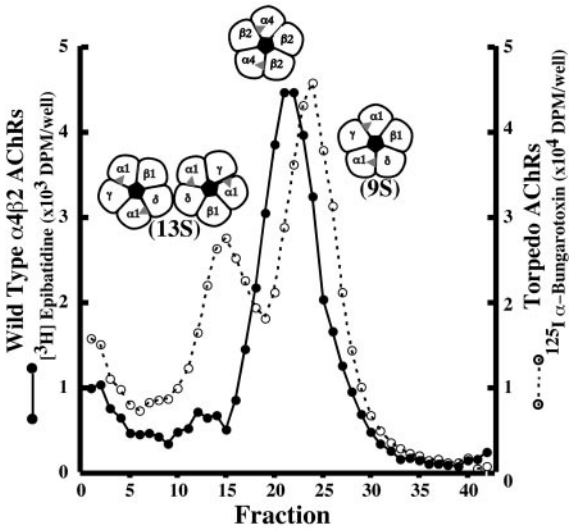

Figure 3. The sucrose gradient sedimentation of wild-type α4β2 AChRs compared with *Torpedo* AChR monopentamers and dipentamers. AChRs solubilized in Triton X-100 were sedimented on 5–20% sucrose gradients. The smaller fraction numbers corresponded to the previous fractions collected from the bottom of the gradient tubes. Near each peak is a symbolic representation of the subunit stoichiometry and organization thought to form the 9 S *Torpedo* AChR monopentamer, 10 S α4β2 monopentamer, or 13 S *Torpedo* AChR dipentamer.

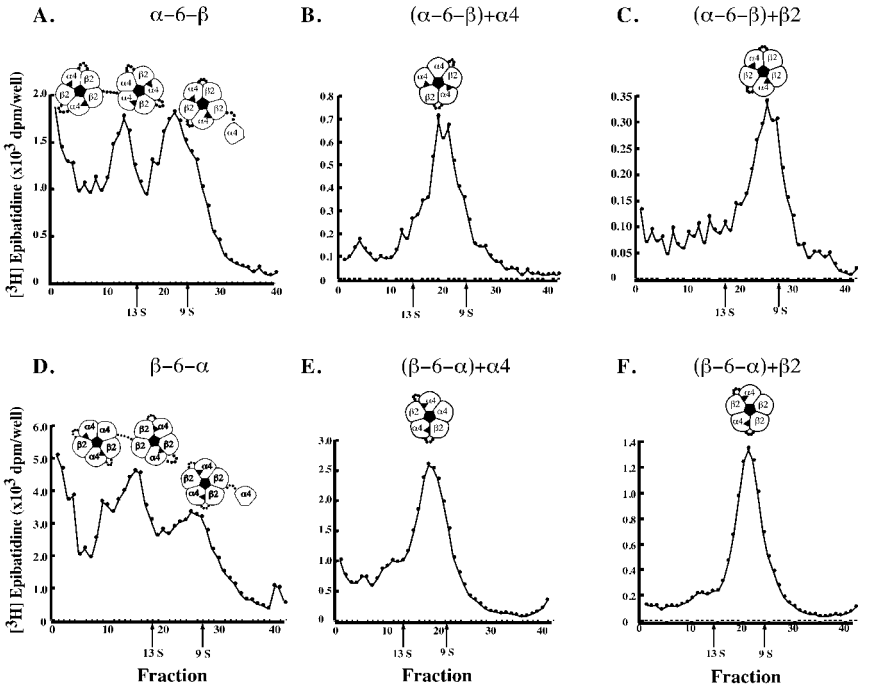

Figure 4. Sucrose gradient sedimentation of concatamers. Arrows indicate the location on internal standards for each gradient of the 9 S monopentamer and 13 S dipentamer peaks of *Torpedo* AChRs. The subunit organization thought to form each of the concatamer AChR peaks is indicated by diagrams above the peaks. *A–F*, The cRNA or combination of cRNAs expressed in that batch of oocytes.

(Hamill et al., 1981), and recordings were performed in ND-96 solution and atropine sulfate (1 μM). The patch pipette contained a solution consisting of the following (in mM): 80 CsF, 20 CsCl, 10 CsEGTA, 10 HEPES, and 3 MgATP, pH 7.2, with CsOH. Channel activation was achieved by isolation of the patch in a continuous stream of agonist solution. All recordings were performed at a holding potential of −80 mV. Data were acquired to video media with a digital data recorder (VR-10A; InstruTech, Great Neck, NY) and standard video cassette recorder. Recordings were sampled at 20 kHz to a personal computer using Axograph 2.0 (Axon Instruments, Foster City, CA) and subsequently analyzed after filtering at 3 kHz (Model 902; 8-pole Bessel; 3 dB; Frequency Devices, Haverhill, MA) using pClamp software (version 6.0.3; Axon Instruments).

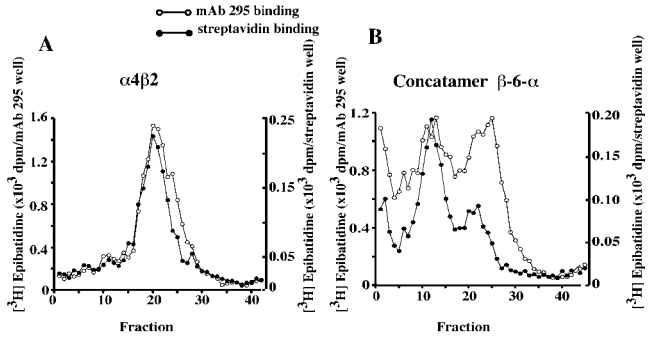

Figure 5. Identification of AChR forms that are expressed on the cell surface. AChRs expressed on the cell surface were labeled with biotin, solubilized in Triton X-100, resolved by sucrose gradient sedimentation, isolated on streptavidin-coated wells, and finally labeled with [3H]epibatidine. Total AChRs were isolated on microwells coated with mAb 295 to β2 subunits. *A*, As expected, the single 10 S form of wild-type α4β2 AChRs was expressed on the cell surface. *B*, The dipentamers formed from β-6-α were selectively expressed on the cell surface. Surprisingly, a small amount of the monopentameric form with a dangling sixth subunit was expressed on the cell surface. Most of the monopentamers formed from concatamers were retained within the cells, probably in the endoplasmic reticulum as a result of exposed retention signals on the unassembled subunit.

Results

Construction of concatamers

Four concatamers (Table 1) were prepared as described in Materials and Methods and Table 1. The concatamer α4-$(AGS)_6$-β2, referred to as α-6-β, was made by linking the C terminus of α4 to the N terminus of β2 using $(AGS)_6$. The concatamer α4-$(AGS)_{12}$-β2, referred to as α-12-β, was made by linking the C terminus of α4 to the N terminus of β2 using $(AGS)_{12}$. The concatamer β2-$(AGS)_6$-α4, referred to as β-6-α, was made by linking the C terminus of β2 to the N terminus of α4 using $(AGS)_6$. The concatamer β2-α4, referred to as β-α, was made by linking the C terminus of β2 directly to the N terminus of α4 without any linker. The original full sequences of the coding region of mature α4 and β2 subunits were conserved in the concatamers. The C-tail of the human α4 subunit, after the final transmembrane domain (M4), had only 8 aa, whereas the C-tail of the β2 subunit after M4 had 23 aa. Therefore, a longer linker was needed to achieve the same total length when linking the short C-terminal region of α4 to the N terminus of β2 than was required to link the longer C-terminal region of β2 to the N terminus of α4 to maintain a similar length between subunits.

Concatamers remain intact during assembly of AChRs

Immunoblots of Triton X-100 extracts from oocytes injected with concatamers confirmed the integrity of expressed proteins (Fig. 1). Concatamer β-6-α migrated at a molecular weight of ~130 kDa, which was quite close to its calculated molecular weight. The detection of double bands suggested that post-translational modifications exist for both AChRs formed by concatamers and wild-type α4β2 subunits. The difference in molecular weight of the two α4 bands reflects the differences in glycosylation and may reflect differences between glycosylation of subunits that have not left the endoplasmic reticulum and those that have passed through the Golgi (data not shown). These data also demonstrated that concatamer cRNAs were properly translated in the oocytes, and no degradation to unlinked subunits was seen. Immunoblot analysis of the other three concatamers showed similar results (data not shown).

Functional assays confirmed the presence of intact concatamers in functional AChRs (Fig. 2). Paradiso et al. (2001) showed that the four C-terminal amino acids of human α4 subunit contribute to the formation of a binding site for 17-β-estradiol, and that binding of this estrogen increased the response to ACh of α4β2 AChRs by several-fold. We confirmed these results with wild-type α4β2 AChRs. In AChRs formed from concatamers in which the C terminus of β2 was linked to the N terminus of α4 (concatamer β-6-α), leaving the C terminus of α4 unaltered, 17-β-estradiol showed a similar allosteric potentiation effect on the ACh response. However, in AChRs formed from concatamers in which the C terminus of α4 was linked to the N terminus of β2 (concatamer α-6-β and α-12-β), thereby altering the C terminus of α4, 17-β-estradiol had no effect on the ACh response.

Concatamers can form dipentamers when expressed alone or monopentamers when expressed with free α4 or β2 subunits

Because AChRs are formed from five subunits, concatamers of two linked subunits could only form monopentamers if the concatamers were coexpressed with free α4 or β2 to permit the assembly of two concatamers with a free subunit to form a functional pentamer. However, concatamers of two subunits, when expressed alone, could assemble into either monopentamers with one dangling subunit or into two linked pentamers if the linkers were long enough to permit it. Experiments described below showed that concatamers with sufficiently long linkers form functional dipentamers, and that coexpression with a free subunit resulted in functional monopentamers, the stoichiometry of which depended on the identity of the free subunit. An inevitable result of forming dipentameric AChRs from linked subunits was that one of the linked AChRs had the stoichiometry $(\alpha4)_2(\beta2)_3$, and the other had the stoichiometry $(\alpha4)_3(\beta2)_2$. Subunit stoichiometry within a pentamer was found to have important consequences, as predicated by previous studies (Zwart and Vijverberg, 1998; Nelson et al., 2003).

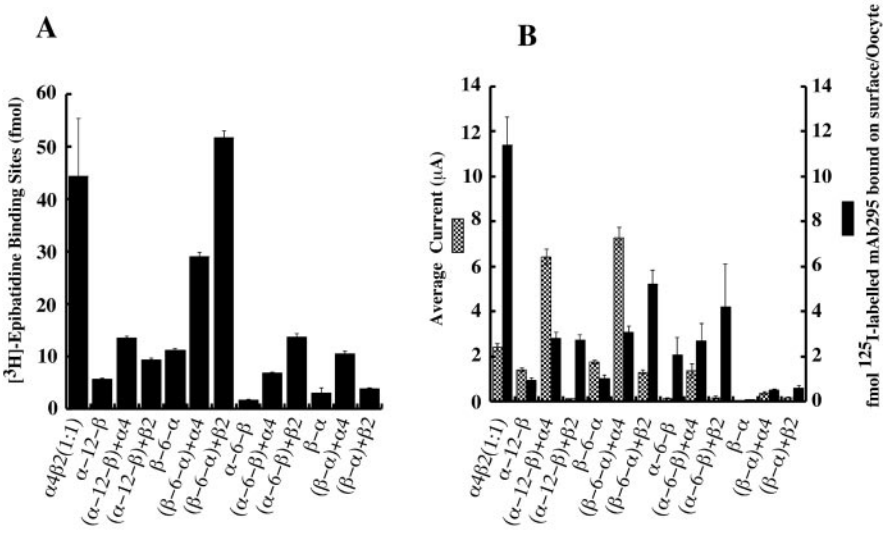

Figure 6. Measurement of total AChR [^{3}H]epibatidine-binding sites, surface AChR-binding sites, and 100 μM ACh-induced currents of the concatamers. Each measurement averages the results from at least two batches of four to five oocytes. The same batch of oocytes was used in both *A* and *B*. Error bars indicate SE. *A*, The total [^{3}H]epibatidine-binding sites immunoisolated per oocyte. *B*, Average current was measured by applying 100 μM ACh to the oocytes. Surface labeling was determined by incubating oocytes in ND-96 solution containing 10% heat-inactivated normal horse serum and 5 nM ^{125}I-mAb 295 for 3 hr at 25°C, followed by washing steps with ND-96 solution to remove nonspecifically bound mAbs.

Sucrose gradient sedimentation indicated that wild-type α4β2 AChRs were monopentamers that sedimented at 10 S, as expected. The molecular weight of α4 (75,000 Da) was much more than that of β2 (49,000 Da) or α1 (38,000 Da) because of the large cytoplasmic domain of the α4 subunit. Thus, α4β2 AChRs sedimented faster than *Torpedo* AChR monopentamers but slower than the dipentamers of *Torpedo* AChRs (Whiting and Lindstrom, 1987; Schoepfer et al., 1988) (Fig. 3). α-6-β and β-6-α sedimented as three components thought to correspond to a pentamer with a dangling linked subunit, a dipentamer, and larger oligomers (Fig. 4*A*,*D*). When free α4 or β2 subunits were coexpressed with these concatamers, only a monopentamer peak remained (Fig. 4*B*,*C*,*E*,*F*). This was also true if α5 was coexpressed (data not shown).

The monopentamers formed from concatamers expressed alone must have contained six subunits rather than five, as in a properly assembled wild-type AChR monopentamer. The slightly slower sedimentation of these monopentamers with a dangling sixth subunit probably resulted from their increased radius of gyration. Biotin-based isolation of surface AChRs demonstrated that monopentamers with a dangling sixth subunit were not as efficiently expressed on the surface as were dipentamers (Fig. 5). This was expected because unassembled AChR subunits were expected to have an exposed endoplasmic reticulum retention signal (Wang et al., 2002). Concatamers with sufficiently long linkers to assemble efficiently into dipentamers with no dangling subunits, β-6-α (Fig. 4*D*) and α-12-β (data not shown), were expressed on the cell surface (Fig. 5) and capable of functioning efficiently (Fig. 6).

Electrophysiological and functional activity of concatamers

In the experiments on expression and function of concatamers, the moles of surface AChRs were measured using ^{125}I-mAb 295 to

Table 2. Surface expression of all concatamers alone and with free α4 or β2 subunits

AChR	Surface AChR (fmol ^{125}I-mAb 295 binding site/oocyte)	Total current[a] (μA)	Specific activity (current/surface AChR) (μA/fmol mAb 295 binding)	Relative specific activity[b] to wild-type α4β2(1:1)
α4β2(1:1)	11.4 ± 1.23	2.42 ± 0.15	0.21	1.0
α-12-β	0.94 ± 0.11	1.39 ± 0.07	1.47	6.9
α-12-β + α4	2.79 ± 0.27	6.42 ± 0.34	2.31	10.9
α-12-β + β2	2.74 ± 0.23	0.11 ± 0.01	0.04	0.2
β-6-α	1.01 ± 0.15	1.75 ± 0.09	1.72	8.1
β-6-α + α4	3.09 ± 0.27	7.29 ± 0.44	2.36	11.1
β-6-α + β2	5.20 ± 0.63	1.30 ± 0.08	0.25	1.2
α-6-β	2.05 ± 0.79	0.13 ± 0.02	0.06	0.3
α-6-β + α4	2.70 ± 0.74	1.38 ± 0.31	0.51	2.4
α-6-β + β2	4.19 ± 1.90	0.17 ± 0.05	0.04	0.2
β-α	0.06 ± 0.01	0.02 ± 0.00	0.27	1.3
β-α + α4	0.49 ± 0.07	0.36 ± 0.05	0.73	3.5
β-α + β2	0.60 ± 0.09	0.16 ± 0.02	0.26	1.2

[a] Measured at 100 μM ACh.

[b] All numbers in the specific activity column were divided by 0.21 [specific activity of α4β2(1:1)].

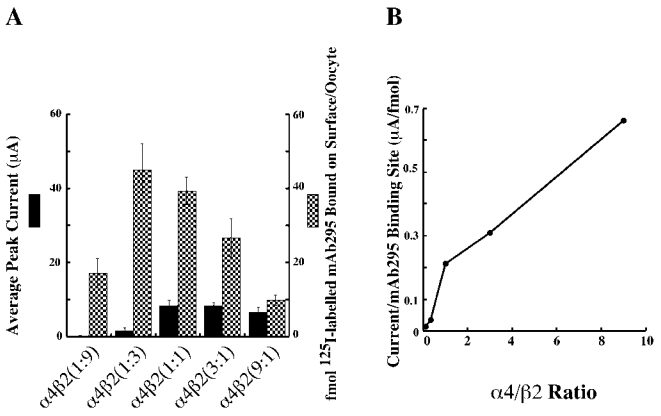

Figure 7. Expression of wild-type $\alpha4\beta2$ AChRs with a different molar ratio of $\alpha4/\beta2$ in *Xenopus* oocytes. *A*, Measurement of surface ^{125}I-mAb 295-binding sites and average peak currents of the AChR formed from wild-type $\alpha4\beta2$ subunits in different $\alpha4/\beta2$ ratios. The 1:9, 1:3, 1:1, 3:1, and 9:1 molar ratios of $\alpha4/\beta2$ RNA were injected with the same total amount of 10 ng. The peak currents were obtained at 300 μM ACh. Surface labeling with 5 nM ^{125}I-mAb 295 was the same as that described in Materials and Methods. *B*, Current per surface ^{125}I-mAb 295-binding site was calculated on the basis of the data in *A*. The more α subunit RNAs were injected, the greater current/surface ^{125}I-mAb 295-binding site was obtained. Each measurement averages the results from at least two batches of 4–10 oocytes. Error bar represents SEM.

label the extracellular surface of $\beta2$ subunits. As a second method for quantifying surface AChRs, labeling by 10 nM [^{3}H]epibatidine for 10 min with or without 1 mM methylcarbamylcholine was used to determine the numbers of surface AChR epibatidine-binding sites as described by Jia et al. (2003). The short incubation with [^{3}H]epibatidine was intended to minimize its accumulation within the oocytes, whereas membrane impermeable methylcarbamylcholine inhibited binding only to surface AChRs. Although the data from this assay suffered from high background relative to specific binding, it confirmed the measures of surface AChRs made using ^{125}I-mAb 295 (data not shown).

α-12-β concatamers (joined by a 50 aa linker) produced functional AChRs (Fig. 6, Table 2). These produced ~57% of the current obtained with an equivalent amount of wild-type $\alpha4\beta2$ (1:1), with 13% of total and 8% of surface binding. The current produced per surface ^{125}I-mAb 295-binding site was approximately sixfold greater with the concatamer than AChRs formed from free subunits at a 1:1 ratio (Table 2). Coexpression of 10 ng of α-12-β mRNA with an additional 5 ng of free $\alpha4$ mRNA increased both the total amount of AChRs and surface expression to 24% of the wild-type $\alpha4\beta2$ (1:1), but current increased to 265%. When coexpressed with $\beta2$ subunits, the total amount of AChRs increased to 21%, surface expression increased to 24%, and current greatly decreased to 4.5% of wild-type $\alpha4\beta2$ (1:1).

β-6-α (joined by a 43 aa linker) expressed alone also formed functional AChRs (Fig. 6, Table 2). These concatamers only produced 25% as many total AChRs and 9% as many surface AChRs but 72% as much current as those of wild-type $\alpha4\beta2$ (1:1). Coexpression of β-6-α with free $\alpha4$ greatly increased the total amount of AChRs to 65%, surface AChRs to 27%, and current to threefold of wild-type $\alpha4\beta2$ (1:1). Coexpression with free $\beta2$ increased the amount of total AChRs to 116% and surface AChRs to 46% of the wild-type $\alpha4\beta2$ (1:1), but the current was reduced.

α-6-β (joined by 32 aa), when expressed alone, formed some functional AChRs but far fewer than did these concatamers with longer linkers (Fig. 6, Table 2). These concatamers produced only 4% as many total AChRs, 18% as many surface AChRs, and 5% of the current as the wild-type $\alpha4\beta2$ (1:1). Thus, this shorter linker severely inhibited both assembly and surface expression. Coexpression with $\alpha4$ greatly increased total AChRs to 15%, surface AChRs to 24%, and current to 57% of wild-type $\alpha4\beta2$ (1:1). The current/surface AChR ratio was increased compared with that of AChRs from concatamer expressed alone. Coexpression with $\beta2$ increased the total AChRs to 31%, surface AChRs to 37%, and current to 7% of the wild-type $\alpha4\beta2$ (1:1).

β-α, with only a 25 aa linker, was unable to form functional AChRs when expressed alone (Fig. 6, Table 2). Total AChRs were only 7% of wild-type $\alpha4\beta2$ (1:1), and there was no expression on the surface. Coexpression with free $\alpha4$ produced 24% of total binding, 4% of surface AChRs, and 15% of current of those from wild-type $\alpha4\beta2$ (1:1). Coexpression with $\beta2$ produced even smaller effects, with an increase in total AChRs to 9%, surface AChRs to 5%, and current to 7% of those from wild-type $\alpha4\beta2$ (1:1). Thus, a 25 aa linker inhibited assembly of subunits, prevented assemblies of subunits that contained some $\alpha4\beta2$ interfaces which could bind epibatidine from getting to the surface, and constrained the orientation between linked subunits. With all concatamers investigated, regardless of their $\alpha4$ to $\beta2$ linkage order or the length of linker, AChRs with possible $(\alpha4)_3(\beta2)_2$ stoichiometry always gave a higher current/surface AChR ratio than those with possible $(\alpha4)_2(\beta2)_3$ stoichiometry.

To determine whether wild-type AChRs in the $(\alpha4)_3(\beta2)_2$ stoichiometry also exhibited higher current/surface AChR, 10 ng of mRNA was expressed, which was comprised of a wide range of ratios of $\alpha4$ to $\beta2$, to favor the formation of either the $(\alpha4)_3(\beta2)_2$ stoichiometry with excess $\alpha4$ or the $(\alpha4)_2(\beta2)_3$ stoichiometry with excess $\beta2$ (Fig. 7). The calculated current/mAb 295 surface-binding site is shown in Figure 7*B*. The more $\alpha4$ subunit mRNA that was injected, the greater current/mAb 295 surface-binding site was obtained. Although, with more $\alpha4$ subunits, the $(\alpha4)_3(\beta2)_2$ stoichiometry was more likely to form. Thus, it was also possible for the $(\alpha4)_3(\beta2)_2$ stoichiometry of wild-type AChRs to produce much more current per surface AChR. It is not known what channel property, such as probability of opening, conductance, open duration, or desensitization rate, accounts for the greater current per surface AChR observed with the $(\alpha4)_3(\beta2)_2$ stoichiometry AChRs.

ACh concentration–response curves

Concentration dependence of activation by ACh of various concatameric AChRs revealed that ACh sensitivities corresponded to

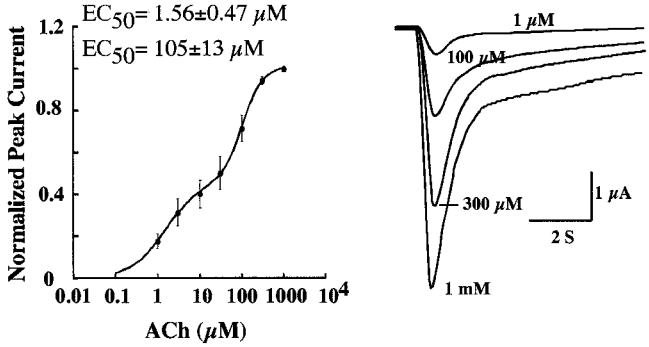

Figure 8. ACh concentration–response curve of concatamer α-12-β was determined. Representative responses to the application of ACh are shown. Different concentrations of ACh were applied to the oocytes at 3 min intervals. Five oocytes were tested, and the responses were normalized to the response at 1000 μM ACh. Each point on the curve represents the mean value. Error bars indicate SEM. The holding potential was set at −50 mV. Two EC_{50} values of 1.56 and 105 μM were identified in this case.

either the $(\alpha4)_2(\beta2)_3$ stoichiometry, $(\alpha4)_3(\beta2)_2$ stoichiometry, or a mixture of the two. Wild-type $\alpha4\beta2$ AChRs expressed in human embryonic kidney cells showed that the $(\alpha4)_2(\beta2)_3$ stoichiometry formed from free subunits had an EC_{50} for ACh of 0.7 μM, whereas the $(\alpha4)_3(\beta2)_2$ stoichiometry formed from free subunits had an ACh EC_{50} of 74 μM (Nelson et al., 2003).

α-12-β dipentamers exhibited a biphasic ACh concentration–response curve with two equal components having EC_{50} values of 1.56 and 105 μM (Fig. 8). Thus, in this concatamer, both the $(\alpha4)_2(\beta2)_3$ stoichiometry (EC_{50} = 1.56 μM) and the $(\alpha4)_3(\beta2)_2$ stoichiometry (EC_{50} = 105 μM) appeared to contribute equally to the ACh response. This concatamer had the longest linker (50 aa between M4 transmembrane domain of $\alpha4$ and the N terminus of $\beta2$) (Table 1) and functioned more efficiently than wild-type $\alpha4\beta2$ (1:1) (Fig. 6, Table 2). With this long linker, there appeared to be little constraint on the function of either AChR in this dipentamer. However, it may be that activation of the more sensitive $(\alpha4)_2(\beta2)_3$ monopentamer often resulted in allosteric activation of the less-sensitive monopentamer mediated through the linker. This could account for the high current per surface AChR of the dipentamer, which is 37-fold that of the $(\alpha4)_2(\beta2)_3$ monopentamer and 64% that of the $(\alpha4)_3(\beta2)_2$ monopentamer (Table 2). Potentiation of $\alpha4\beta2$ AChR function through estradiol acting at the C terminus of $\alpha4$ (Paradiso et al., 2001) is consistent with the idea that linkers through the C terminus might mediate AChR activation. Alternatively, the close packing of the monopentamers within dimers might mediate allosteric interaction independent of action through the linker per se.

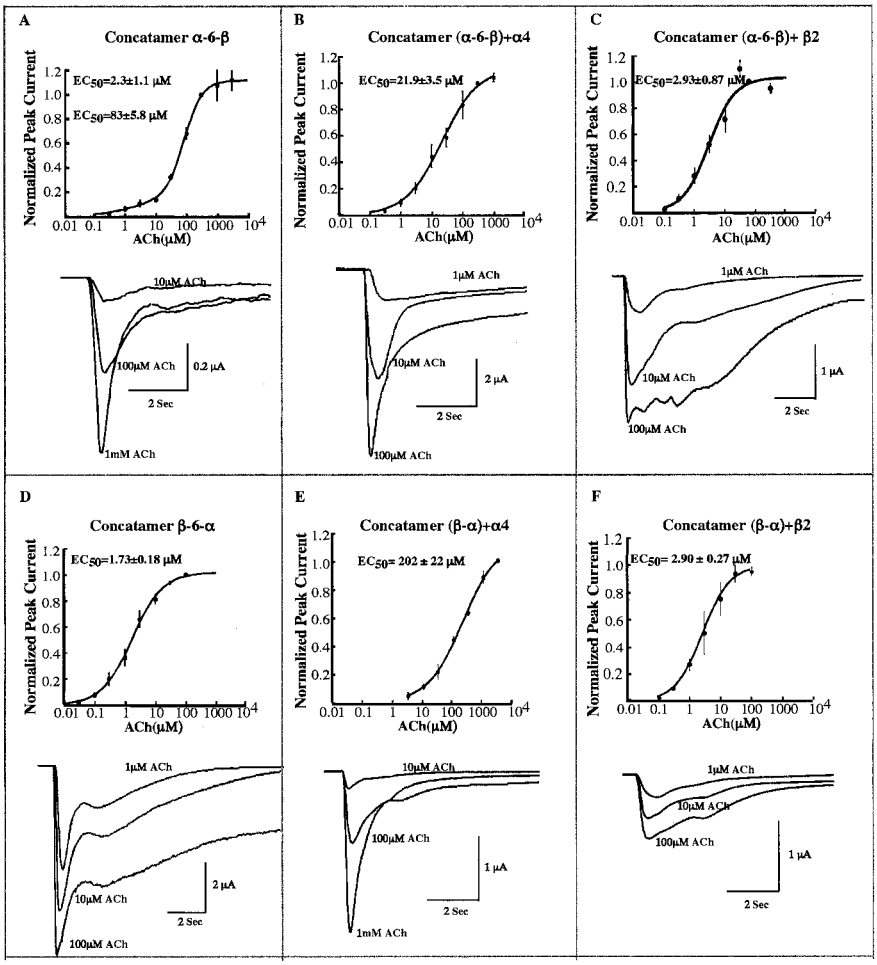

Figure 9. Sensitivity to activation by ACh was determined. A molar ratio of concatamer/α = 1:1 or concatamer/β = 1:1 was used when the concatamers were coexpressed with the wild-type $\alpha4$ or $\beta2$ subunits. Typical responses to the application of ACh are shown. Different concentrations of ACh were applied to the oocytes at 3 min intervals. In the dose–response curve, the responses to ACh were normalized to the response at the ACh concentration, which gave the maximum current for most of the oocytes tested, and each point on the curve represents the normalized mean value from three to six oocytes. Error bars indicate SE. Holding potentials were set at −50 mV. *A–F*, The cRNA or combination of cRNAs expressed in that batch of oocytes.

The β-6-α concatamer exhibited a monophasic ACh concentration–response curve with EC_{50} of 1.7 μM (Fig. 9*D*). Thus, in this concatamer, the $(\alpha4)_2(\beta2)_3$ pentamer appeared to predominate functionally over the $(\alpha4)_3(\beta2)_2$ pentamer. The current–surface AChR was high for AChRs formed in this case (Table 2). Perhaps the 43 aa linker was short enough to mediate a cooperative interaction between the pentamers even more efficiently than the 50 aa linker of α-12-β, so that activation of the more sensitive $(\alpha4)_2(\beta2)_3$ pentamers activated the higher-current $(\alpha4)_3(\beta2)_2$ pentamers completely at ACh concentrations, which fully activated the $(\alpha4)_2(\beta2)_3$ pentamers.

The α-6-β concatamer exhibited a biphasic ACh concentration–response curve with an EC_{50} of 2.3 μM (Fig. 9*A*), accounting for only ≈14% of the response with the $(\alpha4)_2(\beta2)_3$ stoichiometry, and with an EC_{50} of 83 μM, accounting for ≈86% with the stoichiometry of $(\alpha4)_3(\beta2)_2$. This concatamer was very poor at assembling into AChRs, which could bind epibatidine, and this resulted in very low levels of function and function/surface AChR (Fig. 6, Table 2). Subunit assembly, monopentamer function, and cooperative interaction between monopentamers were probably all constrained by the short 32 aa linker (Table 1). Coexpression with free $\alpha4$ resulted in the $(\alpha4)_3(\beta2)_2$ monopentamer (Fig. 4*B*) and a monophasic ACh concentration–response curve with an EC_{50} of 22 μM (Fig. 9*B*). These $(\alpha4)_3(\beta2)_2$ pentamers (Fig. 4*B*) were more sensitive to ACh than wild-type $(\alpha4)_3(\beta2)_2$ pentamers (EC_{50} = 74 μM) (Nelson et al., 2003), presumably as a result of constraints imposed by the linker. Coexpression with free $\beta2$ resulted in $(\alpha4)_2(\beta2)_3$ monopentamers (Fig. 4*C*), with an EC_{50} of 2.9 μM (Fig. 9*C*) approaching that expected of the $(\alpha4)_2(\beta2)_3$ stoichiometry (0.7 μM) (Nelson et al., 2003).

β-α, when expressed alone, could not assemble efficiently to form epibatidine-binding sites, or none of the assembled AChRs reached the cell surface, and consequently there was virtually no function (Fig. 6, Table 2). All of this resulted from the short linker (25 aa) (Table 1). However, a small amount of functional AChRs was detected after coexpression with either free $\alpha4$ or $\beta2$. Coexpression with free $\alpha4$ resulted in $(\alpha4)_3(\beta2)_2$ monopentamers (data not shown) with an EC_{50} for ACh of 202 μM (Fig. 9*E*), approaching that of the wild-type AChR $(\alpha4)_3(\beta2)_2$ stoichiometry. Correspondingly, coexpression with free $\beta2$ subunit resulted in $(\alpha4)_2(\beta2)_3$ monopentamers (data not shown) with a dramat-

ically different EC_{50} of 2.9 μM (Fig. 9*F*), approaching that of the wild-type $(\alpha4)_2(\beta2)_3$ stoichiometry.

Single-channel analysis

Single-channel activities of some of the concatamers were assayed to determine whether linking of the subunits greatly altered kinetics of channel opening. Even a concatamer with a relatively short linker produced normal single-channel activity. Expression levels of the α-6-β concatamer with free α4 and the β-6-α concatamer alone were sufficient for single-channel recordings to be performed. Outside-out patches were formed, and single-channel activity was recorded at −80 mV by isolation of the tip of the recording electrode in a continuously flowing stream of ACh. The comparison between single-channel currents for these AChRs revealed "normal activity" for the AChRs formed from concatamers. In both wild-type and concatamer AChRs, a 2.1 pA (or 26 pS chord conductance) channel predominated. Representative traces for channel activity recorded for each AChR are shown in Fig. 10.

Single-channel currents exhibited two similar amplitudes for all AChRs (Fig. 11). Wild-type α4β2 (1:1) AChRs from injected oocytes exhibited two channel amplitudes of 1.4 ± 0.1 and 2.3 ± 0.1 pA (18 ± 1 and 29 ± 1 pS) (Kuryatov et al., 1997). AChRs from the α-6-β + α4 (thought to be $(\alpha4)_3(\beta2)_2$ monopentamers) (Fig. 4*B*) exhibited two channel amplitudes of 1.5 ± 0.1 and 2.1 ± 0.1 pA that corresponded to 19 ± 1 and 26 ± 1 pS (chord conductances), respectively. AChRs from the β-6-α alone, thought to be dipentamers with one pentamer of each stoichiometry (Figs. 4*D*, 5*B*) but exhibiting ACh sensitivity characteristic of the $(\alpha4)_2(\beta2)_3$ monopentamers (Fig. 9*D*), also had channel amplitudes of 1.7 ± 0.1 and 2.1 ± 0.1 pA, which corresponded to 21 ± 1 and 26 ± 1 pS (chord conductances), respectively.

Channel open-time distributions were best represented by double exponential functions for all AChR activity. The channel kinetics for the predominant larger amplitude channel for both the α-6-β + α4 AChRs and β-6-α alone was similar to the kinetics of wild-type α4β2 AChRs (Fig. 11). There were differences in the kinetics of the less-frequent, lower-amplitude channels. Only the wild-type α4β2 AChRs exhibited long-gating behavior for the lower-amplitude channel (Kuryatov et al., 1997). This was true at both 50 nM and higher ACh concentrations. With concatamers, no great alteration of channel kinetics was detected from single-channel data, which excluded the unlikely possibilities that the functional channels might be composed of tetramers or hexamers, as well as the more likely possibilities that the linker might have altered the conformation changes of the subunits associated with activation and desensitization.

Sites of incorporation of wild-type β subunits in combination with concatamers

If the linkers between α4 and β2 subunits facilitated assembly of the positive side of α4 subunits, distinguished by the protuberance of a loop ending in the disulfide-linked pair of cysteines characteristic of α subunits (Brejc et al., 2001), with the negative side of β2 to form an ACh-binding site at this interface if excess β were expressed with the concatamers, the free β would then be expected to assemble in the position of the β1 subunit of muscle AChRs, which does not participate in forming an ACh-binding site. Alternatively, if the linker within the concatamer was too short or in an unfavorable C′-N′ terminal orientation so that it did not allow assembly of the positive side of α4 with the negative side of β2, then coexpressed excess β subunit might assemble as part of one of the two ACh-binding sites in the AChR. The free β

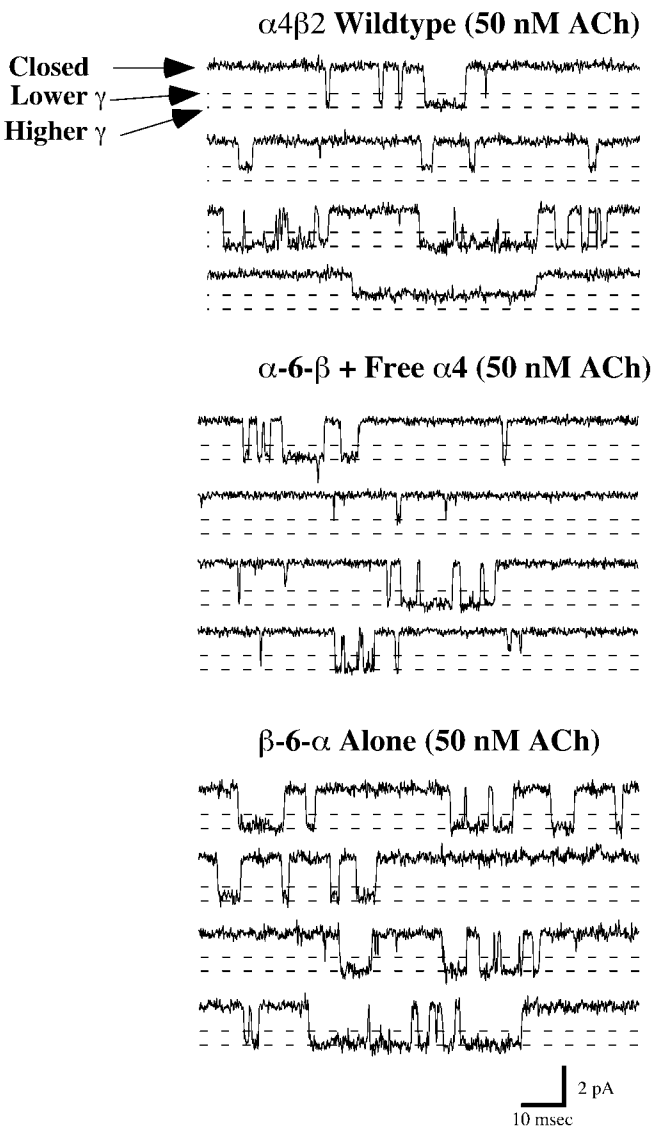

Figure 10. Single-channel currents for AChRs formed from α4β2, α-6-β with free α4, and β-6-α alone. Wild-type AChRs were expressed at a α4:β2 ratio of 1:1. Representative channel activity was recorded in 50 nM ACh at −80 mV. This low concentration of ACh was intended to prevent accumulation of desensitized AChRs. Channel openings of two open amplitudes were observed. The larger ≈2.1 pA opening predominated over the smaller ≈1.5 pA opening.

coexpressed with a α4-β2 concatamer would be expected to assemble at no more than one of the two ACh-binding sites of a closed AChR pentamer, because two α4 subunits are needed to form two ACh-binding sites on a functional AChR. If these were tethered to β2, no more than one free subunit could assemble without causing a dangling, unassembled subunit. The Western blot experiment (Fig. 1) showed that the concatamers were not degraded to form any free subunits, and the biotinylation experiment (Fig. 5) showed that dipentamers formed from subunit concatamers were selectively expressed on the cell surface, while monopentamers with dangling unassembled subunits were selectively retained within the cell.

To establish at which position in an AChR containing tethered subunits a free β would assemble, we investigated assembly with β4 subunits and activation by cytisine. Cytisine was a full agonist on α4β4 AChRs (96 ± 2.0%) (Fig. 12) (Luetje and Patrick, 1991; Papke and Heinemann, 1994) and a weak (5 ± 1.1%) partial

agonist on α4β2 AChRs (Fig. 12). Cytisine was a weak partial agonist when excess free β2 was coexpressed with the concatamers α-6-β, α-12-β, β-α, or β-6-α. The efficacies were 3 ± 0.6, 2 ± 0.4, 3 ± 1, and 4 ± 1%, respectively (Fig. 12). Thus, these AChRs exhibited the characteristic response of α4β2 AChRs, whether the β2 was tethered or free.

α-6-β functioned poorly by itself, and not much better when β2 was coexpressed, but much better when α4 was coexpressed (Table 2, Fig. 6). Addition of either β2 or α4 resulted in the formation of monopentamers instead of dipentamers (Fig. 4). When α-6-β and β4 were coexpressed, cytisine exhibited an efficacy of 52 ± 2% (Fig. 12). This suggested that when the C terminus of α4 was linked to the N terminus of β2 with a short linker, it was difficult to assemble properly to form ACh-binding sites, resulting in low levels of assembly and function (Fig. 6). However, coexpression of this construct with free β4 resulted in efficient assembly at one of the two ACh-binding sites (Figs. 13, 14), resulting in a dramatic increase in efficacy. The efficacy was 52%, compared with 96% for α4β4 AChRs, presumably because only one of the two ACh-binding sites contained β4.

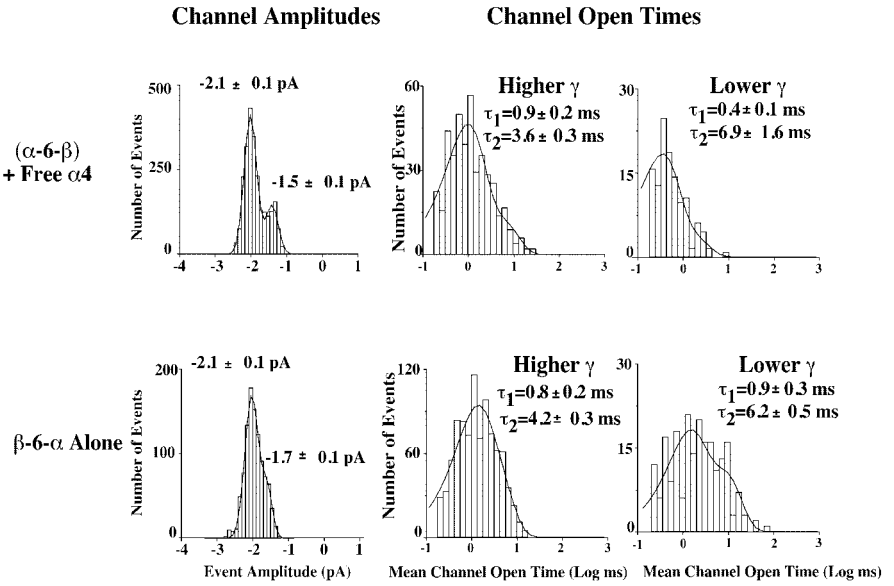

Figure 11. Single-channel properties for AChRs formed from α-6-β with free α4 and β-6-α alone. Single-channel currents exhibited two amplitudes for all AChRs. Representative unitary conductance histograms and channel open-time histograms are shown. The two channel amplitudes of AChRs from wild-type α4β2 are 1.4 ± 0.1 and 2.3 ± 0.1 pA (Kuryatov et al., 1997) and from α-6-β + α4 are 1.5 ± 0.1 and 2.1 ± 0.1 pA, whereas AChRs from the β-6-α alone had channel amplitudes of 1.7 ± 0.1 and 2.1 ± 0.1 pA.

When the linkage was kept in the same orientation from the C terminus of α4 to the N terminus of β2 as in α-6-β, but the length of the linker increased for a total length of 50 aa (from α4 M4 to β2 N terminus) as in α-12-β, the concatamer functioned very well when expressed alone (Table 2, Fig. 6), which suggested that this long linker placed little constraint on the orientation or function of the subunits. When coexpressed with β4, the efficacy of cytisine was 33 ± 2.0%. This suggested that with this long linker, some of the linked α4 and β2 assembled correctly to form ACh-binding sites in between, with the result that β4 assembled in the β1-like position and thus not causing any significant increase in efficacy. Although in the rest of the AChRs, β4 assembled at one of the ACh-binding sites, thereby resulting in some increase in cytisine efficacy.

In β-6-α, the orientation of the linkage was reversed from α-12-β to link the C terminus of β2 to the N terminus of α4. However, because of the long (23 aa) C-terminal sequence of β2, the 18 aa linker resulted in a total of 43 aa between β2 M4 and the N terminus of α4, allowing this concatamer to function well by itself (Table 2, Fig. 6*B*). Coexpression of β-6-α with β4 resulted in a cytisine efficacy of only 10 ± 1% (Fig. 12). With this concatamer, it appears that ACh-binding sites are constrained by the linker to be located at the interfaces of the positive side of α4 with the negative side of β2 within a concatamer (Fig. 13, 14). Most of β4 assembly cannot contribute to a binding site, resulting in only a very small increase in cytisine efficacy.

Coexpression of concatamers with α4 to produce monopentamers with the $(\alpha4)_3(\beta2)_2$ stoichiometry increased the efficacy of cytisine (Fig. 12). This suggested that the conformational changes associated with this stoichiometry not only reduced the potency of ACh but also increased the efficacy of cytisine. The extent of potency increase may have depended on constraints placed by the length of the linker and whether the free α4 subunit assembled at the position equivalent to that of β1 subunits in muscle AChRs (where it does not participate in forming an ACh-binding site), or whether it assembled as part of one of the two ACh-binding sites.

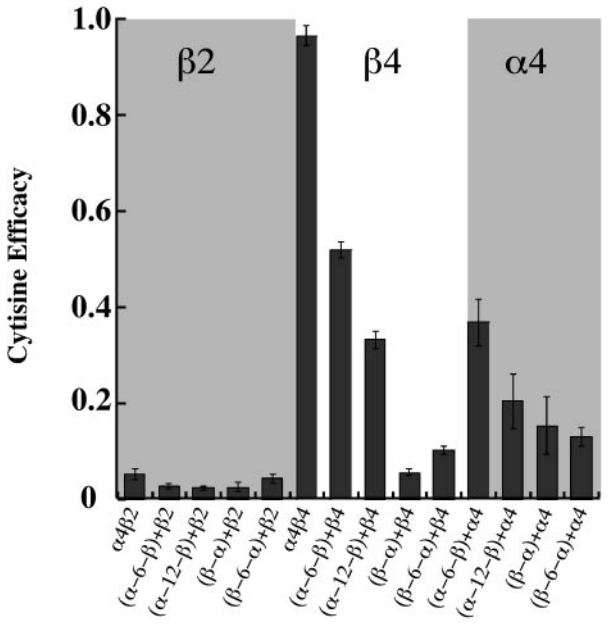

Figure 12. Efficacy of cytisine on AChRs formed by concatamers. Cytisine efficacy was determined by comparing the response to 100 μM cytisine for that oocyte with the response measured for 300 μM ACh, which gave maximum current for all cases. All recordings were performed at a holding potential of −50 mV. Each column represents the mean value of the cytisine efficacy measured from at least two batches of oocytes, and, in each batch, at least four to six oocytes were tested. Cytisine efficacies for α4β4, α-6-β plus β4, and β-6-α plus β4 were 96.5 ± 2, 51.9 ± 1.6, and 10.3 ± 0.9%, respectively.

In α-6-β and α-12-β, the linker extended from the C terminus of α4 near the surface of the membrane to the N terminus of β2

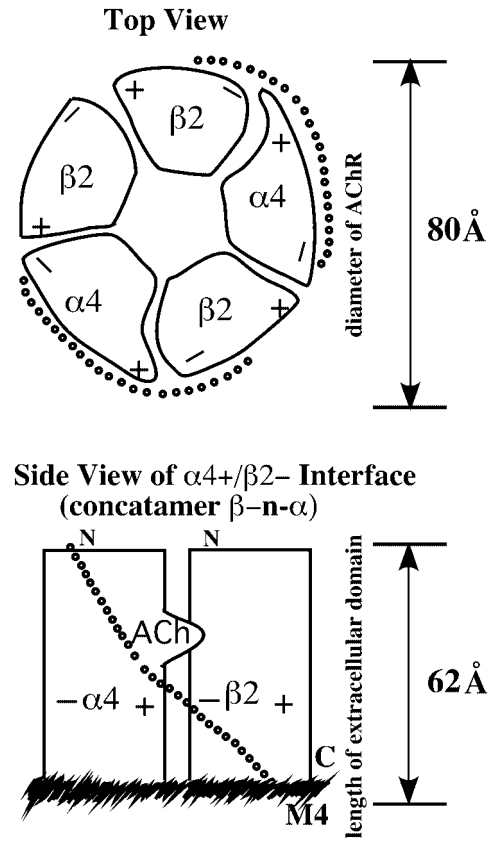

Figure 13. This diagram, which is based on the dimensions and polypeptide chain orientations of the ACh-binding protein (Brejc et al., 2001), shows the extracellular domain of an $\alpha4\beta2$ AChR and possible orientations of a linker between the C terminus near the transmembrane region M4 of one subunit and the N terminus of the adjacent subunit. The N terminus is located at the extracellular tip on the outer edge of the negative side of a subunit (Brejc et al., 2001). The C terminus of M4 is located on the outer surface of the AChR ~10 Å above the lipid bilayer at the border between the largely α helical transmembrane domain and the largely β sheet structure of the extracellular domain (Miyazawa et al., 2003). The height of the extracellular domain is 62 Å, and each subunit is ~47 Å wide (Brejc et al., 2001). The linker must extend from the C terminus of M4 to the N terminus of the adjacent subunit. As shown in the top side view, a linker from the C terminus of $\beta2$ to the N terminus of $\alpha4$ might extend from the M4 transmembrane domain of $\beta2$ across the interface, forming the ACh-binding site to the N terminus on the negative side of $\alpha4$ and thereby facilitating assembly of an ACh-binding site within a concatamer. As shown in the bottom side view, a linker from the C terminus of $\alpha4$ to the N terminus of $\beta2$ might extend from the M4 transmembrane domain of $\alpha4$ across the interface between $\beta2$ and $\alpha4$, which does not form an ACh-binding site, stabilize this interface, and thus promote formation of ACh-binding sites between concatamers. The linker is presumed to be a random coil, according to secondary structure prediction using the sequence analysis software MacVector (International Biotechnologies, New Haven, CT).

located at the top of the negative side of subunits (Brejc et al., 2001). In β-α and β-6-α, the linker extended from the C terminus of $\beta2$ near the surface of the membrane to the N terminus at the top of the negative side of $\alpha4$ (Fig. 13). This suggested that linkage from the C terminus of $\alpha4$ to the N terminus of $\beta2$ might link the interface between the positive side of $\beta2$ and negative side of $\alpha4$ (Fig. 13). If so, the ACh-binding sites, which are known to form at the positive side of α and the negative side of adjacent subunits (Brejc et al., 2001), would have formed between concatamers. Conversely, the linkage from the C terminus of $\beta2$ to the N terminus on the negative side of $\alpha4$ might have linked the interface known to form ACh-binding sites and therefore promoted the formation of ACh-binding sites within concatamers (Fig. 13). If ACh-binding sites were formed within β-α and β-6-α concatamers, free $\beta4$ could not have incorporated easily into an ACh-binding site, thus accounting for the small increase in cytisine efficacy when free $\beta4$ was added to these concatamers. Added free subunits would have incorporated selectively in the site equivalent to $\beta1$ of muscle AChRs. If ACh-binding sites formed between concatamers in the case of α-6-β and α-12-β, this could have accounted for the large increase in efficacy when free $\beta4$ was added.

Discussion

We examined the functional properties, ligand-binding properties, and sedimentation velocity profiles of AChRs formed by linked pairs of $\alpha4$ and $\beta2$ subunits expressed in *Xenopus* oocytes. We demonstrated that it was possible to form functional AChRs from $\alpha4$ and $\beta2$ subunits that were synthesized with peptide linkers joining them from the C terminus of one subunit to the N terminus of the next. Western blot analysis showed that linked subunits remained intact, and this was confirmed by functional studies. The response to ACh of AChRs, formed from concatamers, was potentiated by 17-β-estradiol acting at the binding site, which was formed by the C terminus of $\alpha4$ subunits (Paradiso et al., 2001), if the linker extended from the C terminus of $\beta2$ to the N terminus of $\alpha4$. However, 17-β-estradiol had no effect on AChRs formed from concatamers in which the C terminus of $\alpha4$ was altered by linkage to the N terminus of $\beta2$. Linkage of the subunits reduced the amount of AChRs assembled but increased the ACh-induced current/cell surface AChR when the linker had a length of 43 or 50 aa. A total of 32 aa between the M4 transmembrane domain of one subunit and the N terminus of the next allowed some function. Limiting the effective linker to only 25 aa precluded the assembly of functional AChRs from concatamers alone but allowed function in combination with free subunits (Table 2). Concatamers with 32 aa or more in the linker formed functional dipentamers when expressed alone. Dipentamers were selectively expressed on the cell surface, compared with monopentamers with a dangling sixth subunit, which probably revealed an endoplasmic reticulum retention signal (Wang et al., 2002) on the unassembled subunit. Each dipentamer consisted of one AChR with the subunit stoichiometry $(\alpha4)_2(\beta2)_3$ and another AChR with the stoichiometry $(\alpha4)_3(\beta2)_2$. Coexpression of linked and free subunits resulted in expression of functional monopentameric AChRs with the stoichiometry $(\alpha4)_2(\beta2)_3$ in the case of free $\beta2$, $(\alpha4)_3(\beta2)_2$ in the case of free $\alpha4$, or $(\alpha4)_2(\beta2)_2(\beta4)$ in the case of free $\beta4$. Whether they were formed from linked subunits and a free subunit, or all free subunits, the $(\alpha4)_3(\beta2)_2$ stoichiometry produced more ACh-induced current per surface AChR than did the $(\alpha4)_2(\beta2)_3$ stoichiometry. The $(\alpha4)_3(\beta2)_2$ stoichiometry was less sensitive to ACh than the $(\alpha4)_2(\beta2)_3$ stoichiometry. Dipentamers produced currents per

surface AChR approaching that of the $(\alpha4)_3(\beta2)_2$ stoichiometry, perhaps as a result of cooperative activation of the less sensitive $(\alpha4)_3(\beta2)_2$ pentamer resulting from activation of the more sensitive $(\alpha4)_2(\beta2)_3$ pentamer. Single-channel studies showed that linkage of subunits did not greatly alter the amplitude and duration of channel opening. Linkage between the C terminus of $\beta2$ near the lipid bilayer and the N terminus at the top of the negative side of $\alpha4$ appeared to promote formation of ACh-binding sites at $\alpha4 + \beta2$ interfaces within concatamers. Thus, $\beta4$ added free was inefficient at assembling into ACh-binding sites in these concatamers. Conversely, linkage between the C terminus of $\alpha4$ and the N terminus of $\beta2$ appeared to promote formation of ACh-binding sites between concatamers, allowing efficient assembly of free $\beta4$ at ACh-binding sites to increase the efficacy of cytisine. Figure 13 depicts the extracellular structure of an AChR formed from pairs of linked subunits, and Figure 14 summarizes the subunit arrangements and stoichiometries that best account for our data.

Variable stoichiometries of $\alpha4\beta2$ AChRs result from the homologous nature of AChR subunits. Although all AChR subunits share many of the same structural features, resulting from their evolution from a primordial homomeric AChR, individual subunits have evolved specializations for particular functional roles. $\beta1$, $\beta3$, and $\alpha5$ subunits appear to assemble only at the position in a pentamer that is not part of an ACh-binding site but that is formed between the positive side of a δ, $\beta2$, or $\beta4$ subunit and the negative side of an $\alpha1$-$\alpha6$ subunit. $\beta2$ and $\beta4$ subunits can assemble both in the $\beta1$-like position and as part of an ACh-binding site formed between the positive side of an $\alpha2$, 3, 4, or 6 subunit and the negative side of $\beta2$ or $\beta4$. The existence of the $(\alpha4)_3(\beta2)_2$ stoichiometry shows that $\alpha4$ subunits can also compete for assembly in the $\beta1$-like position. In Figure 7, it was observed that when large excesses of $\beta2$ or $\alpha4$ subunits were expressed, the total amount of surface AChR was decreased. This might result from competition of subunits to assemble stoichiometries that are either not structurally stable or unable to function because they have only one ACh-binding site [e.g., $(\alpha4)_1(\beta2)_4$ or $(\alpha4)_4(\beta2)_1$].

Torpedo dipentameric AChRs are linked by a disulfide bond between the penultimate C-terminal cysteine of their δ subunits to produce an effective linker between the two monopentamers of ~52 aa (Karlin, 2002). It has been reported that dipentamers of *Torpedo* AChRs undergo synchronous cooperative activation (Schindler et al., 1984). This might resemble the cooperative activation of low-sensitivity $(\alpha4)_3(\beta2)_2$ monopentamers by activation of high-sensitivity $(\alpha4)_2(\beta2)_3$ monopentamers, which might account for the monotonic ACh concentration–response curve of β-6-α (Fig. 9) and the high current/surface AChR of dipentamers (Table 2).

The original incentive for studies of linked subunits was the observation that the truncated extracellular domain of $\alpha7$ AChR subunits did not assemble efficiently into homopentamers (Wells et al., 1998). We thought that linking the truncated extracellular domains might improve the efficiency of assembly, because the crystal structure of the ACh-binding protein has been determined (Brejc et al., 2001). It is a pentamer of 80 Å diameter, similar to the assembled extracellular domain of $\alpha7$ AChRs. It is not yet clear what structural adaptations permit it to assemble efficiently as a soluble protein. However, it provides an excellent model for many basic features of AChR structure and a model for understanding the basic dimensions involved in linking the C

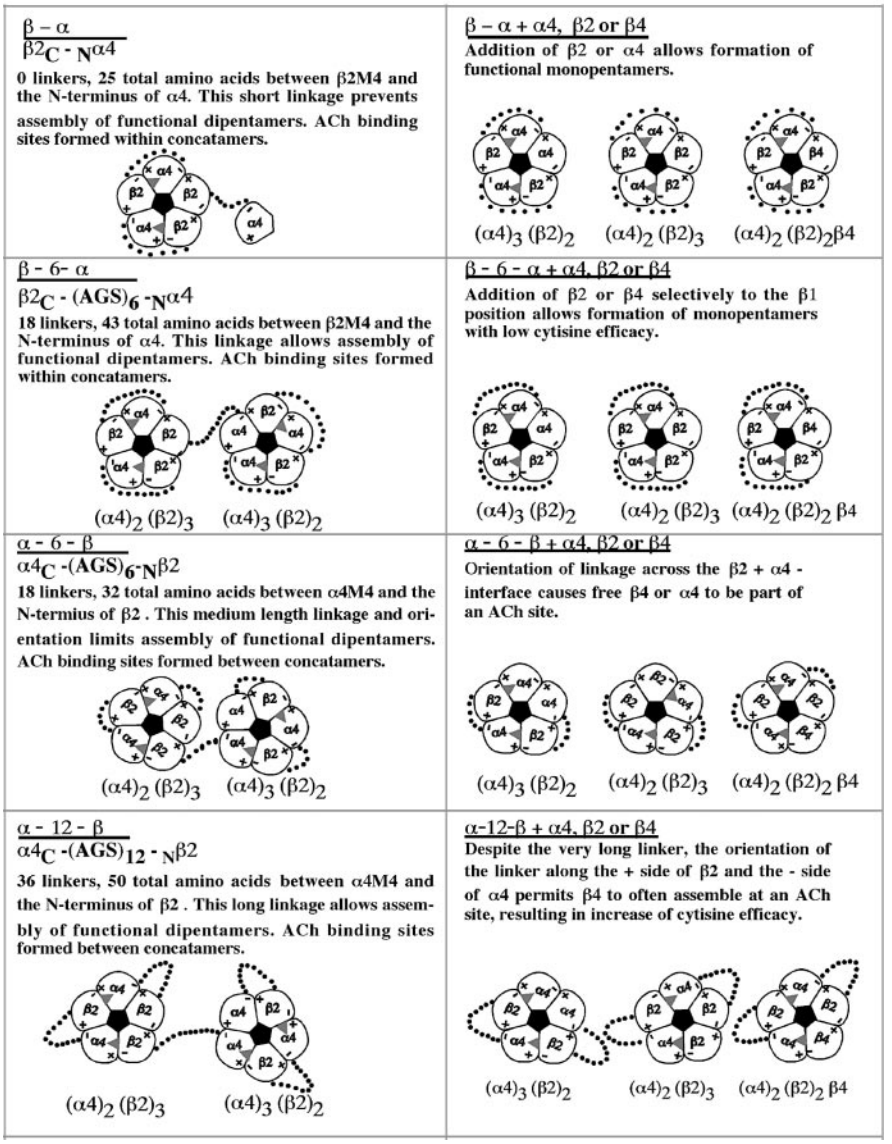

Figure 14. Diagramatic representation of the AChRs thought to be formed by concatamers in combination with wild-type subunits. When the concatamers were expressed alone, both monopentamers and dipentamers were formed. The monopentamer is composed of three pairs of linked subunits, with one subunit dangling off the closed pentamer. This form is selectively retained within the cell. The dipentamer is composed of five pairs of linked subunits forming two pentamers and joined by one pair of linked subunits. One of the pentamers within the dipentamer has the stoichiometry $(\alpha4)_2(\beta2)_3$, and the other pentamer has the stoichiometry $(\alpha4)_3(\beta2)_2$. When concatamers were coexpressed with a free α or β subunit, only closed monopentamers were formed. These consisted of two pairs of linked subunits and one free subunit.

terminus of one subunit (located ≈10 Å above the extracellular surface of the membrane) (Miyazawa et al., 2003) to the N terminus of the adjacent subunit (located at the extracellular tip of the adjacent subunit 62 Å above the transmembrane domain) (Brejc et al., 2001). It would be interesting to investigate whether $\alpha7$ AChR extracellular domains linked into pentameric concatamers would assemble efficiently. This may prove useful in designing water-soluble extracellular AChR domains for structural studies. Linkers between all of the subunits in a pentamer of soluble extracellular domains might ensure efficient assembly in the endoplasmic reticulum lumen, thereby avoiding the usual need for membrane association by at least one transmembrane domain for efficient assembly (Wells et al., 1998). In addition, linkage of all intact subunits within a functional AChR pentamer could define the subunit organization and stoichiometry.

Studies of linked $\alpha4$ and $\beta2$ AChR subunits provide additional examples of functional AChRs with both $(\alpha4)_2(\beta2)_3$ and $(\alpha4)_3(\beta2)_2$ stoichiometries, which extend beyond the recognition of the properties of a mixture of these two stoichiometries expressed in a transfected cell line (Nelson et al., 2003). The possibility that both stoichiometries occur in the brain, reflect different functional roles, and are differentially subject to regulation by exposure to nicotine (Kim et al., 2003; Nelson et al., 2003) suggests that such plasticity in stoichiometry warrants additional investigation.

References

Anand R, Lindstrom J (1990) Nucleotide sequence of the human nicotinic acetylcholine receptor $\beta2$ subunit gene. Nucleic Acids Res 18:4272.

Anand R, Conroy WG, Schoepfer R, Whiting P, Lindstrom J (1991) Neuronal nicotinic acetylcholine receptors expressed in *Xenopus* oocytes have a pentameric quaternary structure. J Biol Chem 266:11192–11198.

Anand R, Bason L, Saedi MS, Gerzanich V, Peng X, Lindstrom J (1993) Reporter epitopes: a novel approach to examine transmembrane topology of integral membrane proteins applied to the $\alpha1$ subunit of the nicotinic acetylcholine receptor. Biochemistry 32:9975–9984.

Brejc K, van Dijk WJ, Klaassen RV, Schuurmans M, van Der Oost J, Smit AB, Sixma TK (2001) Crystal structure of an ACh-binding protein reveals the ligand-binding domain of nicotinic receptors. Nature 411:269–276.

Cooper E, Couturier S, Ballivet M (1991) Pentameric structure and subunit stoichiometry of a neuronal nicotinic acetylcholine receptor. Nature 350:235–238.

Gerzanich V, Anand R, Lindstrom J (1994) Homomers of $\alpha8$ and $\alpha7$ subunits of nicotinic receptors exhibit similar channel but contrasting binding site properties. Mol Pharmacol 45:212–220.

Gerzanich V, Peng X, Wang F, Wells G, Anand R, Fletcher S, Lindstrom J (1995) Comparative pharmacology of epibatidine: a potent agonist for neuronal nicotinic acetylcholine receptors. Mol Pharmacol 48:774–782.

Hamill OP, Marty A, Neher E, Sakmann B, Sigworth FJ (1981) Improved patch-clamp techniques for high-resolution current recording from cells and cell-free membrane patches. Pflügers Arch 391:85–100.

Hurst RS, Kavanaugh MP, Yakel J, Adelman JP, North RA (1992) Cooperative interactions among subunits of a voltage-dependent potassium channel. Evidence from expression of concatenated cDNAs. J Biol Chem 267:23742–23745.

Im WB, Pregenzer JF, Binder JA, Dillon GH, Alberts GL (1995) Chloride channel expression with the tandem construct of $\alpha6$-$\beta2$ $GABA_A$ receptor subunit requires a monomeric subunit of $\alpha6$ or $\gamma2$. J Biol Chem 270:26063–26066.

Isacoff EY, Jan YN, Jan LY (1990) Evidence for the formation of heteromultimeric potassium channels in *Xenopus* oocytes. Nature 345:530–534.

Jia L, Flotildes K, Li M, Cohen BN (2003) Nicotine trapping causes the persistent desensitization of $\alpha4\beta2$ nicotinic receptors expressed in oocytes. J Neurochem 84:753–766.

Karlin A (2002) Emerging structure of the nicotinic acetylcholine receptors. Nat Rev Neurosci 3:102–114.

Kim H, Flanagin BA, Qin C, Macdonald RL, Stitzel JA (2003) The mouse *Chrna4* A529T polymorphism alters the ratio of high to low affinity $\alpha4\beta2$ nAChRs. Neuropharmacology 45:345–354.

Kuryatov A, Gerzanich V, Nelson M, Olale F, Lindstrom J (1997) Mutation causing autosomal dominant nocturnal frontal lobe epilepsy alters Ca^{2+} permeability, conductance, and gating of human $\alpha4\beta2$ nicotinic acetylcholine receptors. J Neurosci 17:9035–9047.

Kuryatov A, Olale FA, Choi C, Lindstrom J (2000a) Acetylcholine receptor extracellular domain determines sensitivity to nicotine-induced inactivation. Eur J Pharmacol 393:11–21.

Kuryatov A, Olale F, Cooper J, Choi C, Lindstrom J (2000b) Human $\alpha6$ AChR subtypes: subunit composition, assembly, and pharmacological responses. Neuropharmacology 39:2570–2590.

Liman ER, Tytgat J, Hess P (1992) Subunit stoichiometry of a mammalian K^+ channel determined by construction of multimeric cDNAs. Neuron 9:861–871.

Luetje CW, Patrick J (1991) Both α- and β-subunits contribute to the agonist sensitivity of neuronal nicotinic acetylcholine receptors. J Neurosci 11:837–845.

Methfessel C, Witzemann V, Takahashi T, Mishina M, Numa S, Sakmann B (1986) Patch clamp measurements on *Xenopus laevis* oocytes: currents through endogenous channels and implanted acetylcholine receptor and sodium channels. Pflügers Arch 407:577–588.

Miyazawa A, Fujiyoshi Y, Unwin N (2003) Structure and gating mechanism of the acetylcholine receptor pore. Nature 424:949–955.

Nelson ME, Lindstrom J (1999) Single channel properties of human $\alpha3$ AChRs: impact of $\beta2$, $\beta4$ and $\alpha5$ subunits. J Physiol (Lond) 516:657–678.

Nelson ME, Kuryatov A, Choi CH, Zhou Y, Lindstrom J (2003) Alternate stoichiometries of $\alpha4\beta2$ nicotinic acetylcholine receptors. Mol Pharmacol 63:332–341.

Papke RL, Heinemann SF (1994) Partial agonist properties of cytisine on neuronal nicotinic receptors containing the $\beta2$ subunit. Mol Pharmacol 45:142–149.

Paradiso K, Zhang J, Steinbach JH (2001) The C terminus of the human nicotinic $\alpha4\beta2$ receptor forms a binding site required for potentiation by an estrogenic steroid. J Neurosci 21:6561–6568.

Schindler H, Spillecke F, Neumann E (1984) Different channel properties of *Torpedo* acetylcholine receptor monomers and dimers reconstituted in planar membranes. Proc Natl Acad Sci USA 81:6222–6226.

Schoepfer R, Whiting P, Esch F, Blacher R, Shimasaki S, Lindstrom J (1988) cDNA clones coding for the structural subunit of a chicken brain nicotinic acetylcholine receptor. Neuron 1:241–248.

Tzartos S, Hochschwender S, Vasquez P, Lindstrom J (1987) Passive transfer of experimental autoimmune myasthenia gravis by monoclonal antibodies to the main immunogenic region of the acetylcholine receptor. J Neuroimmunol 15:185–194.

Wang F, Gerzanich V, Wells GB, Anand R, Peng X, Keyser K, Lindstrom J (1996) Assembly of human neuronal nicotinic receptor $\alpha5$ subunits with $\alpha3$, $\beta2$, and $\beta4$ subunits. J Biol Chem 271:17656–17665.

Wang JM, Zhang L, Yao Y, Viroonchatapan N, Rothe E, Wang ZZ (2002) A transmembrane motif governs the surface trafficking of nicotinic acetylcholine receptors. Nat Neurosci 5:963–970.

Wells GB, Anand R, Wang F, Lindstrom J (1998) Water-soluble nicotinic acetylcholine receptor formed by $\alpha7$ subunit extracellular domains. J Biol Chem 273:964–973.

Whiting P, Lindstrom J (1986) Pharmacological properties of immunoisolated neuronal nicotinic receptors. J Neurosci 6:3061–3069.

Whiting P, Lindstrom J (1987) Purification and characterization of a nicotinic acetylcholine receptor from rat brain. Proc Natl Acad Sci USA 84:595–599.

Whiting PJ, Lindstrom JM (1988) Characterization of bovine and human neuronal nicotinic acetylcholine receptors using monoclonal antibodies. J Neurosci 8:3395–3404.

Zoli M, Le Novere N, Hill Jr JA, Changeux JP (1995) Developmental regulation of nicotinic ACh receptor subunit mRNAs in the rat central and peripheral nervous systems. J Neurosci 15:1912–1939.

Zwart R, Vijverberg HP (1998) Four pharmacologically distinct subtypes of $\alpha4\beta2$ nicotinic acetylcholine receptor expressed in *Xenopus laevis* oocytes. Mol Pharmacol 54:1124–1131.